Nuclear Instruments and Methods in Physics Research B 393 (2017) 44–48

Contents lists available at ScienceDirect

Nuclear Instruments and Methods in Physics Research B

journal homepage: www.elsevier.com/locate/nimb

Defect production in Ar irradiated graphene membranes under different initial applied strains

J. Martinez-Asencio [a,*], C.J. Ruestes [b], E. Bringa [b], M.J. Caturla [a]

[a] Dept. Física Aplicada, Facultad de Ciencias, Fase II, Universidad de Alicante, Alicante E-036090, Spain
[b] CONICET and Facultad de Ciencias Exactas y Naturales, Universidad Nacional de Cuyo, Mendoza 5500, Argentina

ARTICLE INFO

Article history:
Received 1 September 2016
Received in revised form 12 September 2016
Accepted 30 September 2016
Available online 7 October 2016

Keywords:
Molecular dynamics
Graphene
Defects
Irradiation

ABSTRACT

Irradiation with low energy Ar ions of graphene membranes gives rise to changes in the mechanical properties of this material. These changes have been associated to the production of defects, mostly isolated vacancies. However, the initial state of the graphene membrane can also affect its mechanical response. Using molecular dynamics simulations we have studied defect production in graphene membranes irradiated with 140 eV Ar ions up to a dose of 0.075×10^{14} ions/cm^2 and different initial strains, from −0.25% (compressive strain) to 0.25% (tensile strain). For all strains, the number of defects increases linearly with dose with a defect production of about 80% (80 defects every 100 ions). Defects are mostly single vacancies and di-vacancies, although some higher order clusters are also observed. Two different types of di-vacancies have been identified, the most common one being two vacancies at first nearest neighbours distance. Differences in the total number of defects with the applied strain are observed which is related to the production of a higher number of di-vacancies under compressive strain compared to tensile strain. We attribute this effect to the larger out-of-plane deformations of compressed samples that could favor the production of defects in closer proximity to others.

1. Introduction

Graphene [1], a single layer of graphite, has been considered one of the most promising discoveries in materials science due to its novel and interesting properties arising from its 2D nature and its electronic [2], optical [3], thermodynamic [4] and mechanical properties [5]. It is one of the strongest materials, despite being flexible and light-weighted, with an experimental Young's modulus of 1.0 ± 0.1 TPa [5]. These structural and physical properties make graphene a really suitable candidate for the development of new electronic devices like transistors [6], sensors [7], energy storage systems [8] or even components for space exploration [9], among many others.

These properties can be modified, or even improved, in the presence of defects. One way of introducing defects intentionally in a controlled manner is by ion implantation. Recent experiments using irradiation with 140 eV Ar ions have shown that the mechanical properties of graphene depend strongly on irradiation dose [10]. For a very low defect content (around 0.2%), counter-intuitively, graphene increases its elastic modulus to approximately 1.6 TPa and becomes stiffer than the pristine structure. At high doses, however, the elastic modulus decreases, as expected. This behavior has been explained by the presence of mono-vacancies formed during irradiation [10,11]. In a previous work, we have shown that the initial strain of the graphene membrane also plays an important role in the mechanical properties of this material and its behavior after irradiation [12]. In fact, besides irradiation, changes in the mechanical properties of graphene can also be induced by applying different strains [13]. We have shown that the out-of-plane displacements that are intrinsic to graphene [14] are modified both by the applied strain and by the irradiation. In fact, the mechanical response of irradiated graphene is due to, not only the formation of defects, but also to the changes of these out-of-plane displacements induced by the irradiation [12].

The types of defects produced by irradiation in free standing graphene have been studied by different groups using molecular dynamics simulations [15–19]. For example, Bellido and Seminario performed radiation damage simulations using C ions with energies ranging between 0.1 eV and 100 keV [15]. They observed the formation of mono-vacancies and di-vacancies for energies above 30 eV. After the molecular dynamics simulations, the atomic structures of the defects were optimized using DFT, revealing a 5-9 structure for the mono-vacancies and a 5-8-5 structure for the di-vacancies. In this work, we focus on the production of defects in graphene membranes with different initially applied strains,

* Corresponding author.
E-mail address: jesusmartinez@ua.es (J. Martinez-Asencio).

http://dx.doi.org/10.1016/j.nimb.2016.09.033
0168-583X/

from −0.25% (compressive strain) to 0.25% (tensile strain). The question we want to address is if the initial applied strain influences defect production during irradiation. In our work we examine the formation of vacancies, their content and type, resulting from low energy irradiation of a graphene sample with Ar ions under different initial strain conditions.

2. Methodology

We have performed molecular dynamics (MD) simulations of low energy Ar ions irradiation on a graphene drumhead at 300 K using the classical MD code LAMMPS [20]. Our simulations consist of a circular graphene membrane containing 674644 C atoms within a 75 nm radius and non-periodic boundary conditions. Our sample is divided into an outermost annulus 1 nm thick which contains fixed atoms in order to achieve a suspended system, an inner annulus of 2 nm with a Langevin thermal bath, to keep a constant temperature of 300 K, and a dynamical region for the rest of the drumhead. The main aim of this thermal bath region is producing a smooth thermodynamical transition between the dynamical and the immobile regions.

A hybrid Tersoff/ZBL [21] potential was used to simulate the 3-body C–C interactions of the graphene membrane. Also, the empirical ZBL potential was used for the Ar-Ar and the Ar-C interactions. This potential, developed by Ziegler-Biersack–Littmarck [22] mimics a repulsive Coulombic potential with a screening function, which is essential for properly describing the short-range interactions between the ions and the atoms of the system that take place during an irradiation simulation.

Firstly, we performed a minimization of the system using the conjugate gradient algorithm [23]. Then, the sample and the simulation box were both relaxed using the NPH ensemble ($P = 0$ bars in the x and y directions) for 3 ps using a timestep of 1 fm. Now, we begin the irradiation of our graphene membrane with low energy (140 eV) Ar ions. During the irradiation, the NVE ensemble was switched on. The irradiation was performed perpendicularly to the sample, along the z-direction, whose implantation region was defined as a circle of 65 nm radius from the center of the drumhead. A total of 1000 Ar ions were shot to random targets within that region, 1 ion every 5000 timesteps. In this case a variable timestep was defined to have a proper integration of the equations of motion for short range interactions. Finally, the system is relaxed for another 35 ps.

As a consequence of the ion implantation, defects of different nature are produced on the membrane. Defect production detection and analysis has been carried out using the open visualization tool OVITO [24]. A first nearest neighbor analysis with a cutoff of 1.7 Angstroms is considered. The average C–C distance for flat graphene is 1.42 Angstroms and 2.46 Angstroms for second neighbours. However, our cutoff was set to a value between those quantities due to the existence of wrinkles on our membrane, which could stretch the C–C bonds providing a slightly larger value for the first neighbor distance than the expected one for the flat graphene case. Those intrinsic ripples emerge due to thermal fluctuations on the out-of-plane direction, given a finite temperature, 300 K in this case. With this method, the coordination number of each atom is obtained. In order to visualize the defects, those atoms with coordination 3 are removed, and only atoms with adjacent vacancies remain. These atoms are grouped in clusters of defects. Defects are also identified using OVITO and are then classified as mono-vacancies, di-vacancies and higher order vacancy clusters (more than two vacancies).

The same above mentioned simulations and analysis were also done for samples with different initial strains, from −0.25% (compressive) to 0.25% (tensile). These new atom positions are remapped fitting its new simulation box size.

Using MD (LAMMPS) with the Tersoff potential [25], the formation energies of the observed vacancy structures are also obtained. We performed an energy minimization of a small pristine graphene sample of 2.7 nm × 2.5 nm with 264 C atoms and also for graphene flakes of this same size containing either a mono-vacancy, or a di-vacancy or a higher order vacancy (tri-vacancy) with the configurations obtained in the irradiated samples.

3. Results

Defect production under different applied strains is presented in Fig. 1. Fig. 1(a) shows the total number of vacancies produced as a function of dose for all applied strains. In all cases the number of defects increases linearly with dose and the total number of defects is very similar for all applied strains. In Fig. 1(b) the number of vacancies with dose is divided between those in mono-vacancies, in di-vacancies and in larger order clusters for two different applied strains, a compressive strain of −0.15% and a tensile strain of 0.15%. Here a difference is observed in the number of di-vacancies, with a higher production of these defects for the case of a compressive strain.

The differences in the number of defects produced in the case of compressive strain versus tensile strain are more clearly seen in Fig. 2. Fig. 2(a) shows the difference in the total number of vacancies produced in a compressive strain of −0.15% and a tensile strain of 0.15% as a function of dose. This difference increases with dose, with higher defect production in the case of the compressive strain. In the same figure, the difference in the number of mono-vacancies and di-vacancies as a function of dose is also presented. It is interesting to see how as the dose increases, the differences for di-vacancies increases, with a compressive strain having more di-vacancies than a tensile strain, while the opposite occurs for mono-vacancies. This trend is observed for all the cases studied here except for the highest applied strain (−0.25% and 0.25%).

The increased formation of di-vacancies in compressed samples can be attributed to the changes in the out-of-plane displacements induced by the irradiation in the case of compressive strain compared to tensile strain. Fig. 2(b) shows the value of the minimum z coordinate for all atoms in the membrane as a function of dose for the case of −0.15% (solid squares) and 0.15% (open circles). The differences are quite remarkable. While no changes are observed in the tensile sample, the compressed membrane shows deeper and deeper values of the z component. In fact, a deep well is formed in the compressed membrane for the highest dose studied. In Fig. 2(c) we can observe differences between the distribution and amplitude of the wavelength of the ripples created in the initial strained structure and the resulting deep well formed on the sample due to irradiation effects.

The structure of the defects identified in the simulations after irradiation is presented in Fig. 3. Fig. 3(a) is a mono-vacancy, Fig. 3(b) and (c) are the two types of di-vacancies formed, a di-vacancy at first nearest neighbours (Fig. 3(b)), and a di-vacancy at second nearest neighbours (Fig. 3(c)). Fig. 3(d) shows a tri-vacancy. We have calculated the formation energies of these different defects. For the case of the mono-vacancy a formation energy of 6.88 eV has been obtained, in agreement with simulations performed by other authors with this potential [25] and close to the values obtained experimentally [26] and to the lowest value obtained using density functional theory (6.8–8.0 eV) [27–29]. For the di-vacancy, the formation energy of the configuration of Fig. 3(b) is 9.18 eV, which is higher than the values obtained with DFT (8.08 eV) [30,31]. For the case of the di-vacancy in the configuration of Fig. 3(c) a much higher formation energy is obtained,

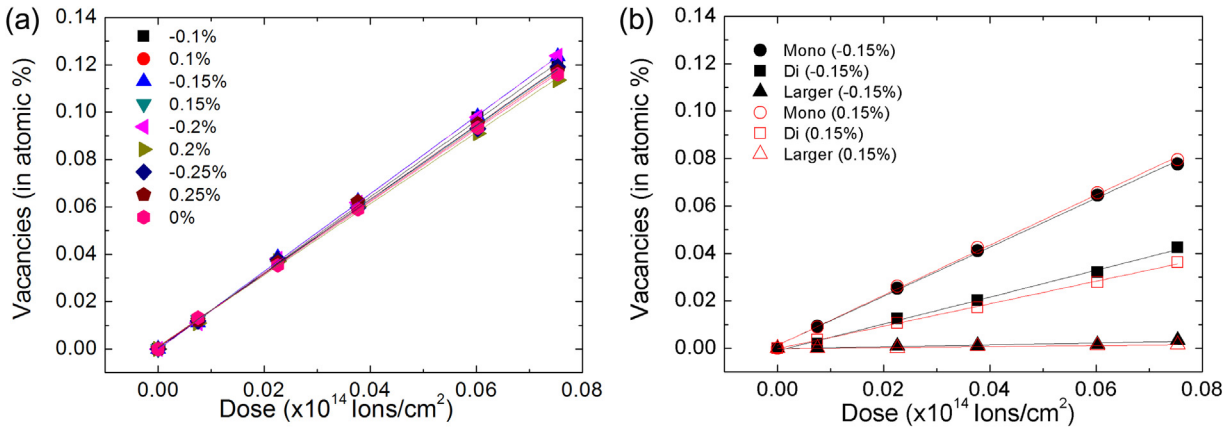

Fig. 1. Defects produced in the graphene layer as a function of dose (a) total number of vacancies (in atomic %) for all the strains calculated (b) mono-vacancies, di-vacancies and higher order clusters for two different applied strains, −0.15% (compressive) and 0.15% (tensile).

13.93 eV. This structure is, therefore, thermodynamically much less favourable than the di-vacancy at first nearest neighbours, but can be formed dynamically during the irradiation, although with a much lower probability. We have performed an annealing

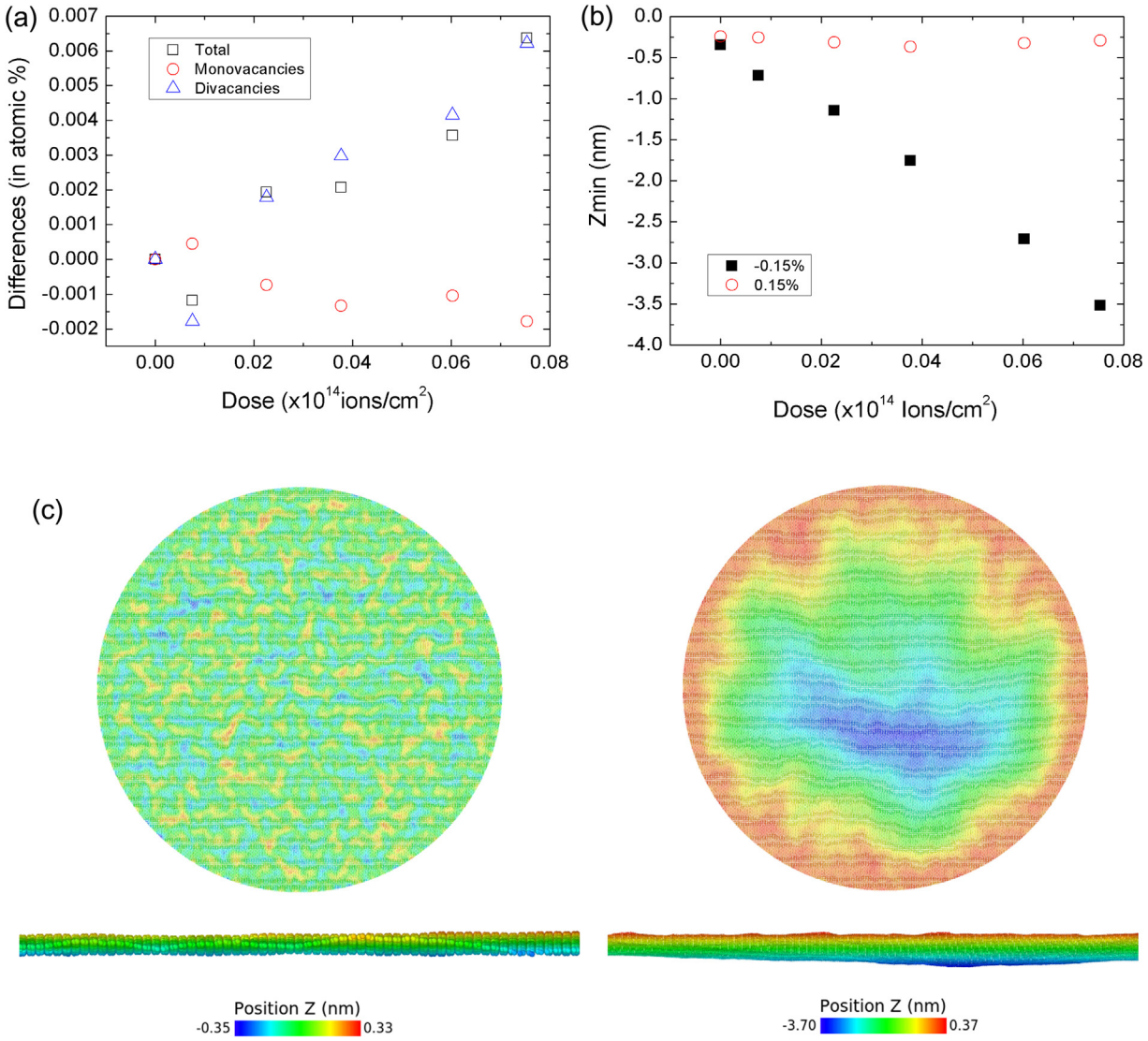

Fig. 2. (a) Difference between the number of defects produced as a function of dose between an initial applied strain of −0.15% and one of 0.15% (b) Minimum value of the z component of the atoms in the membrane as a function of dose for −0.15% and 0.15% initially applied strain (c) on the left, frontal and side view of the topography of the membrane before irradiation. On the right, frontal and side view after irradiation for a dose of 0.075×10^{14} atoms/cm^2.

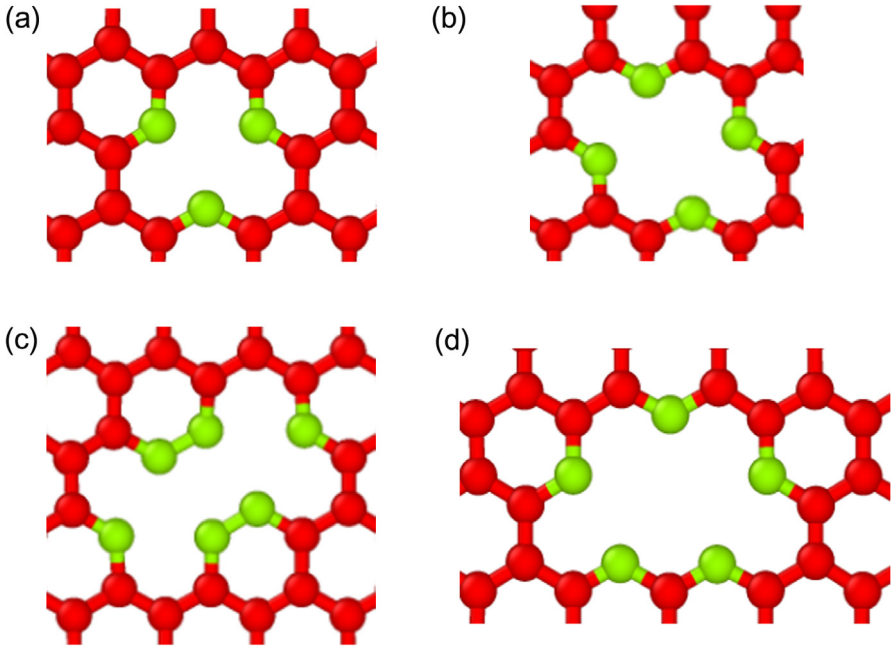

Fig. 3. Most common defects obtained in the irradiation of graphene with Ar 150 eV ions (a) mono-vacancy (b) di-vacancy at first nearest neighbours (c) di-vacancy at second nearest neighbours (d) triple-vacancy. Green (light) are atoms with coordination 2, red (dark) are atoms with coordination 3. Image obtained with OVITO [24]. (For interpretation of the references to colour in this figure legend, the reader is referred to the web version of this article.)

of the structure of Fig. 3(c) at 500 K for 0.2 ns but no modifications in the configuration have been observed for this timescale. Finally, for the case of the tri-vacancy (Fig. 3(d)), a formation energy of 11.5 eV is obtained, which is a bit higher than the DFT value of 10.63 eV [29].

Fig. 4(a) presents the concentration of the two types of di-vacancies identified for all different strains and the highest dose simulated, 0.075×10^{14} ions/cm^2. Most of the di-vacancies formed are at first nearest neighbours distance and only a few are at second nearest neighbour, which is in agreement with the higher stability of the former. Note also that, as mentioned above, under compressive strain the number of di-vacancies is slightly higher than under tensile strain. We attribute this behavior to the out-of-plane distortions of the membrane. The higher deformation of the graphene layer when it is under a compressive strain could favor the production of close-by defects.

As mentioned above, the higher production of defects for compressive strain and particularly of di-vacancies could be attributed to the changes in out-of-plane displacements produced in the membrane during irradiation. Fig. 4(b) shows the minimum value of the z component of all atoms in the membrane after irradiation at the highest dose studied and for all the different initial strains applied. Interestingly, when the membrane is under tension no significant changes are observed in the out-of-plane displacements, the membrane remains mostly in a plane with slight corrugations. However, when the membrane is under compressive strain we can observe important differences in the out-of-plane displacements. The membrane is no longer on a plane but it forms a deep well, with depths of several Angstroms as shown in Fig. 4(b), as well as Fig. 2(b). This shape could be responsible for higher defect production and enhanced di-vacancy formation in initially compressed samples.

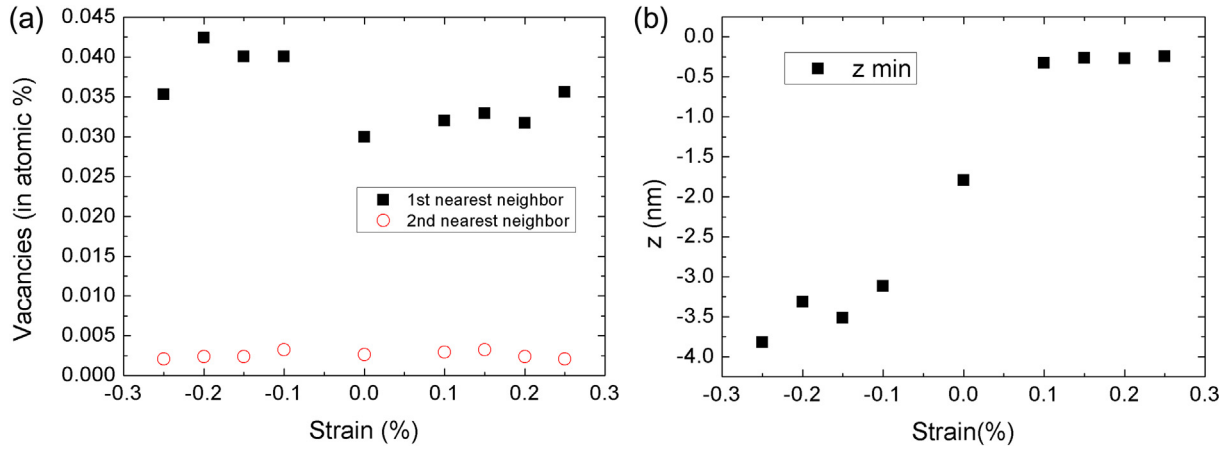

Fig. 4. (a) Number of di-vacancies as a function of applied strain for a dose of 0.075×10^{14} ions/cm^2. Open symbols are di-vacancies at second nearest neighbours distance while filled symbols are di-vacancies at first nearest neighbours distance (b) Minimum value of the z component of the atoms in the membrane for different applied strains after irradiation (same dose as in (a)).

4. Conclusions

We have studied the formation of defects in graphene membranes due to irradiation with 140 eV Ar ions for different initial applied strains using molecular dynamics with empirical potentials. Our simulations show that the total number of defects produced increases linearly with dose for all cases. Defects produced are mono-vacancies, di-vacancies and, with a much lower frequency, higher order vacancy clusters (triple-vacancies in particular). The initial strain influences the total number of defects produced and, specially, the type of defect formed. Under compressive strain the total number of defects is slightly higher than under tension for the same dose. More significantly, the number of mono-vacancies is lower when a compressive strain is applied and the formation of di-vacancies is favored. We attribute these differences to the out-of-plane deformations induced by the irradiation. In the case of tensile strain no changes are observed while in the case of compressive strain a deep well is formed due to the irradiation which would favor the formation of defects in close proximity.

Acknowledgements

Simulations were performed in the computer cluster and other computer resources of the Dept. of Applied Physics at the UA as well as in the supercomputer MareNostrum at Barcelona Supercomputing Center - Centro Nacional de Supercomputación (The Spanish National Supercomputing Center). This work is supported by the Generalitat Valenciana through grant reference PROMETEO2012/011 and the Spanish government through grant FIS2010-21883. CJR and EMB thank support from SeCTyP-UNCuyo and ANPCyT grant PICT-2014-0696.

References

[1] K.S. Novoselov, A.K. Geim, S.V. Morozov, D. Jiang, Y. Zhang, S.V. Dubonos, I.V. Grigorieva, A.A. Firsov, Science 306 (2004) 666–669.
[2] K.S. Novoselov, Z. Jiang, Y. Zhang, S.V. Morozov, H.L. Stormer, U. Zeitler, J.C. Maan, G.S. Boebinger, P. Kim, A.K. Geim, Science 315 (2007) 1379.
[3] Y.W. Son, M.L. Cohen, S.G. Louie, Nature 444 (2006) 347–349.
[4] S. Ghosh, I. Calizo, D. Teweldebrhan, E.P. Pokatilov, D.L. Nika, A.A. Balandin, W. Bao, F. Miao, C.N. Lau, Appl. Phys. Lett. 92 (2008) 151911.
[5] C. Lee, X.D. Wei, J.W. Kysar, J. Hone, Science 321 (2008) 385.
[6] M.C. Lemme, T.J. Echtermeyer, M. Baus, H. Kurz, IEEE Electron Device Lett. 28 (2007) 282–284.
[7] N.L. Rangel, J.A. Seminario, Phys. Chem. A 112 (2008) 13699–13705.
[8] Q. He, H.G. Sudibya, Z. Yin, S. Wu, H. Li, F. Boey, W. Huang, P. Chen, H. Zhang, ACS Nano 4 (2010) 3201–3208.
[9] X. Fan, L. Wang, Sci. Rep. 5 (2015) 12734.
[10] G. López-Polín, C. Gómez-Navarro, V. Parente, F. Guinea, M.I. Katsnelson, F. Pérez-Murano, J. Gómez-Herrero, Nat. Phys. 11 (2015) 26–31.
[11] D.G. Kvashnin, P.B. Sorokin, J. Phys. Chem. Lett. 6 (2015) 2384.
[12] J. Martinez-Asencio, C. Ruestes, E.M. Bringa, M.J. Caturla, Phys. Chem. Chem. Phys. 18 (2016) 13897–13903.
[13] G. López-Polín, M. Jaafar, F. Guinea, R. Roldán, C. Gómez-Navarro, J. Gómez-Herrero, arXiv:1504.05521, (2015).
[14] D. Yoon, Y.-W. Son, H. Cheong, Nano Lett. 11 (2011) 3227–3231.
[15] P. Bellido, J.M. Seminario, J. Phys. Chem. C 116 (2012) 4044–4049.
[16] J. Martinez-Asencio, M.J. Caturla, Nucl. Instr. Meth. B 352 (2015) 225–228.
[17] W. Li, L. Liang, S. Zhao, S. Zhang, J. Xue, J. Appl. Phys. 114 (2013) 234304.
[18] Y. Asayama, M. Yasuda, K. Tada, H. Kawata, Y. Hirai, J. Vac. Sci. Technol., B 30 (2012) 06FJ02.
[19] A.V. Krasheninnikov, K. Nordlund, J. Keinonen, Phys. Rev. B 65 (2002) 165423.
[20] S.J. Plimpton, Comput. Phys. 117 (1995) 1–19.
[21] Devanathan et al., J. Nucl. Mater. 253 (1998) 47.
[22] F. Ziegler, J.P. Biersack, U. Littmark, The stopping and range of ions in solids, Pergamon Press, New York, 1985.
[23] E. Polak, G. Ribiere, Rev. Fr. d'Informatique et de Recherche Opérationelle 16 (1969) 35–43.
[24] A. Stukowski, Modell. Simul. Mater. Sci. Eng. 18 (2010) 015012, http://ovito.org/.
[25] J. Tersoff, Phys. Rev. Lett. 61 (1988) 2879.
[26] P.A. Thrower, R.M. Mayer, Phys. Status Solidi A 47 (1978) 11.
[27] A. Santana, A.M. Popov, E. Bichoutskaia, Chem. Phys. Lett. 557 (2013) 80–87.
[28] H. Zhang, M. Zhao, X. Yang, H. Xia, X. Liu, Y. Xia, Diamond Relat. Mater. 19 (2010) 1240.
[29] A.V. Krasheninnikov, P.O. Lehtinen, A.S. Foster, R.M. Nieminen, Chem. Phys. Lett. 418 (2006) 132.
[30] M.T. Luck, L.D. Carr, Phys. Rev. Lett. 100 (2008) 17550.
[31] H. Zhang, M. Zhao, X. Yang, H. Xia, X. Liu, Y. Xia, Diamond Relat. Mater. 19 (2010) 1240.